Atmospheric Circulation Change in a Warming Climate: Hemispheric Asymmetry, ENSO Variability, and Polar Vortex Weakening

Anish Dhamija

Abstract

Large-scale atmospheric circulation moves heat from the tropics toward the poles and plays a major role in shaping regional climate. I examine multidecadal changes in tropospheric overturning cells, winter stratospheric variability, and tropical Pacific dynamics using ERA5 reanalysis data and nonlinear dimensionality-reduction methods. From 1979 to 2025, the Hadley cell widens at a statistically significant rate, mainly due to shifts in the Southern Hemisphere. During the same period, the Polar cell contracts, again primarily in the Southern Hemisphere, while the Ferrel cell shows no clear long-term trend. These results show that recent circulation changes are not evenly distributed between hemispheres. In the winter stratosphere, diagnostics at 10 hPa and 60°N, including zonal wind, polar-cap geopotential height, and planetary wave-1 amplitude, display strong year-to-year variability but no statistically significant long-term trend. This suggests that internal variability remains the dominant influence on Arctic winter stratospheric behavior over this time range. For the tropics, I construct a low-dimensional nonlinear representation of ENSO using principal component analysis followed by autoencoder embedding. The reconstructed structure broadens and shifts over time, indicating changes in both ENSO strength and spatial pattern.

Introduction

Earth's climate system is organized by large-scale atmospheric circulation patterns that redistribute heat from the equator toward the poles. The three primary overturning cells in each hemisphere, the Hadley, Ferrel, and Polar cells play a central role in shaping global temperature, precipitation, and storm tracks [4]. Changes in the structure of these circulation cells can therefore influence regional climate extremes, drought patterns, and midlatitude weather variability.

One of the most widely discussed circulation changes in recent decades is the expansion of the Hadley cell. Observational and modeling studies have reported poleward shifts of the subtropical dry zones and widening of the tropical belt [7, 10]. Proposed drivers include greenhouse gas forcing, stratospheric ozone depletion, and internal variability [8, 3]. However, hemispheric asymmetry in these trends remains an open question, and the degree to which changes are monotonic versus variability-driven is still debated.

At higher latitudes, the winter stratospheric polar vortex is a key dynamical feature. The vortex consists of strong westerly winds that encircle the pole and act as a barrier between cold polar air and midlatitudes [12]. Variations in vortex strength are closely linked to planetary wave forcing from the troposphere and can influence surface weather patterns on subseasonal to seasonal timescales [1]. Although some studies have suggested possible weakening of the Arctic vortex in a warming climate, long-term trends remain uncertain because internal variability is large [2].

In the tropics, El Niño–Southern Oscillation (ENSO) represents the dominant mode of interannual climate variability. ENSO events alter global temperature and precipitation patterns and interact with extratropical circulation [11]. Dimensionality-reduction techniques such as principal component analysis and neural-network embeddings offer a framework for studying ENSO as motion on a low-dimensional space [6].

Understanding how tropical variability, midlatitude circulation, and stratospheric dynamics evolve and how they interact is essential for interpreting climate change signals. This study examines (1) multidecadal changes in the Hadley, Ferrel, and Polar cells, (2) long-term behavior of winter stratospheric vortex diagnostics, and (3) structural evolution of ENSO variability using a low-dimensional nonlinear representation. By combining reanalysis data with dynamical diagnostics and machine-learning tools, we aim to clarify which observed changes reflect systematic trends and which are dominated by internal variability.

Methods

Data Sources

We use the ERA5 reanalysis produced by the European Centre for Medium-Range Weather Forecasts (ECMWF) [5]. ERA5 provides a dynamically consistent reconstruction of the global atmosphere by assimilating observations into a numerical weather prediction model using advanced data assimilation techniques.

For tropospheric circulation analysis, we use monthly mean wind and geopotential height fields from 1979 to 2025. For stratospheric diagnostics, we analyze winter (December–January–February; DJF) data at 10 hPa and 60°N, a commonly used level and latitude for monitoring Northern Hemisphere polar vortex variability [1, 12].

For ENSO analysis, we use historical tropical Pacific sea surface temperature (SST) anomaly data covering 1900–2024, based on gridded observational reconstructions [9]. SST anomalies are defined relative to a climatological baseline to isolate variability from the mean seasonal cycle.

Identification of Atmospheric Circulation Cells

To identify the Hadley, Ferrel, and Polar cells, we compute the zonal-mean mass streamfunction at 500 hPa, denoted Ψ_{500}. The mass streamfunction describes large-scale meridional overturning circulation. Zero crossings of Ψ_{500} indicate transitions between circulation cells.

For each year, we determine:

- The latitudinal edges of the Hadley cell,
- The boundaries between the Ferrel and Polar cells,
- The widths of each circulation cell.

Annual means are calculated to reduce seasonal variability. Linear trends are estimated using ordinary least squares regression. Statistical significance is assessed using standard p-values.

To better visualize long-term behavior, we also compute 5-year running means.

Stratospheric Diagnostics

Winter stratospheric variability is analyzed using three standard diagnostics:

1. **Zonal-mean zonal wind at 10 hPa and 60°N**, which measures the strength of the polar vortex.
2. **Polar-cap geopotential height anomalies**, averaged north of 60°N. These heights are dynamically linked to vortex strength through thermal wind balance.
3. **Planetary wave-1 amplitude**, calculated from the zonal Fourier decomposition of geopotential height fields. Wave-1 represents the largest-scale longitudinal disturbance and is a primary mechanism by which tropospheric waves influence the stratosphere.

Anomalies are computed relative to the 1979–2025 climatology. Linear trends are again estimated using ordinary least squares regression. Composite maps of strong and weak vortex years are constructed by selecting years in the upper and lower terciles of DJF zonal wind anomalies.

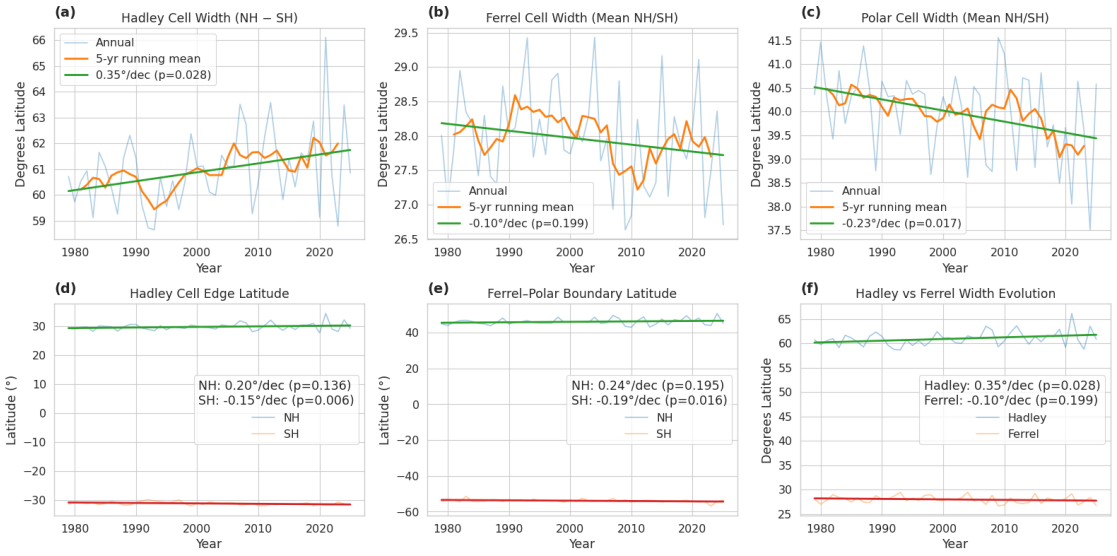

Figure 1: Long-term changes in major atmospheric circulation cells from 1979 to 2025 using ERA5 reanalysis data. Panels (a–c) show the annual-mean widths of the Hadley, Ferrel, and Polar cells. Panels (d–e) show the latitude of the Hadley cell edge and the boundary between the Ferrel and Polar cells in both hemispheres. Panel (f) directly compares the widths of the Hadley and Ferrel cells. Thin lines represent yearly values, thick lines show 5-year running averages to highlight longer-term patterns, and straight lines indicate linear trends estimated using ordinary least squares regression.

Low-Dimensional Reconstruction of ENSO Dynamics

To analyze ENSO variability, we first reduce the dimensionality of tropical Pacific SST anomaly fields using Principal Component Analysis (PCA). PCA identifies orthogonal spatial patterns that explain the largest fraction of variance.

We retain the leading principal components that together explain more than 95% of the variance. These components are then used as input to a nonlinear autoencoder neural network. The autoencoder compresses the data into a three-dimensional latent space (z_1, z_2, z_3) and reconstructs the original SST patterns from this reduced representation.

The latent coordinate z_1 is strongly correlated with the El Niño and therefore represents ENSO amplitude. The remaining coordinates capture additional structure, such as variations in zonal SST gradients.

Phase-space plots of (z_1, z_2) are constructed for different historical periods to examine changes in ENSO circulation. Time series of the latent variables are analyzed to identify long-term shifts in variability amplitude and spatial structure.

Trend Estimation and Statistical Testing

All linear trends are estimated using ordinary least squares regression. Statistical significance is assessed using two-sided t-tests on regression slopes. Reported uncertainties correspond to one standard error of the estimated trend.

Where appropriate, smoothing using 5-year running means is applied for visualization purposes only; statistical analyses are performed on unsmoothed data.

Results

Changes in Large-Scale Atmospheric Circulation

Figure 1 shows how the major atmospheric circulation cells have changed from 1979 to 2025 using ERA5 reanalysis data. We identify the boundaries of the Hadley, Ferrel, and Polar cells using the Ψ_{500} mass streamfunction and analyze annual averages.

The Hadley cell, which dominates tropical circulation, has widened at a rate of $0.35 \pm 0.31°$ latitude per decade ($p = 0.028$; Fig. 1a). However, this widening is not evenly split between hemispheres. The Southern Hemisphere plays the larger role: its Hadley edge shifts equatorward at $-0.15 \pm 0.10°$ per decade ($p = 0.006$), while the Northern Hemisphere boundary shows a small and statistically insignificant poleward shift ($0.20 \pm 0.26°$ per decade; $p = 0.136$; Fig. 1d). This means the expansion of tropical circulation is mainly driven by changes south of the equator.

The Ferrel cell, which lies in the midlatitudes, does not show a clear long-term trend (Fig. 1b). Its width changes by $-0.10 \pm 0.16°$ per decade ($p = 0.199$), which is not statistically significant. This suggests that midlatitude overturning circulation has remained relatively stable during this period.

The Polar cell behaves differently. It contracts at a rate of $-0.23 \pm 0.19°$ per decade ($p = 0.017$; Fig. 1c). Again, the Southern Hemisphere dominates this signal. The Ferrel–Polar boundary shifts equatorward at $-0.19 \pm 0.16°$ per decade ($p = 0.016$; Fig. 1e), while the Northern Hemisphere shows no significant trend. Taken together, these results suggest that recent circulation changes are stronger and more consistent in the Southern Hemisphere.

Winter Stratosphere: Variability vs. Long-Term Trends

Figure 2 focuses on winter (DJF) conditions in the stratosphere at 10 hPa and 60°N. Panel (a) shows zonal-mean zonal wind anomalies, which measure the strength of the polar vortex. The linear trend is slightly negative (-0.60 m s^{-1} per decade; $p = 0.574$), but it is not statistically significant. Instead, the dominant feature is strong year-to-year variability, with wind anomalies often exceeding ± 10 m s^{-1}.

Panel (b) shows polar-cap geopotential height anomalies. These are physically linked to vortex strength: when the vortex weakens, heights tend to increase. The trend here is also not statistically significant (-0.76 per decade; $p = 0.438$), and large fluctuations are visible from one winter to the next.

Panel (c) presents planetary wave-1 amplitude, which measures how strongly waves from the troposphere disturb the stratosphere. Although a small positive trend appears ($+0.89$ per decade; $p = 0.752$), it is not statistically significant.

These three diagnostics tell a consistent story: the winter stratosphere shows strong variability from year to year, but no clear long-term trend over the 1979–2025 period.

What Strong and Weak Polar Vortex States Look Like

Figure 3 helps visualize this variability. During strong vortex years (Figs. 3a–b), the polar region is surrounded by a nearly circular band of strong westerly winds. This symmetric structure indicates a stable and well-centered vortex.

During weak vortex years (Fig. 3c), the pattern changes dramatically. Westerly winds weaken or even reverse in some regions, and the vortex becomes distorted and shifted away from the pole. The structure becomes asymmetric, especially over Eurasia. These patterns are typical of winters influenced by strong planetary wave activity.

The difference between these states highlights how dynamic and flexible the winter stratosphere can be.

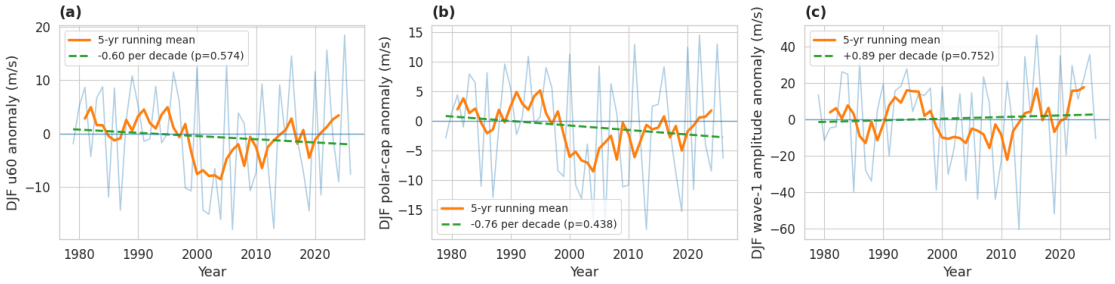

Figure 2: Winter (DJF) stratospheric conditions at 10 hPa and 60°N from 1979 to 2025. (a) Zonal-mean zonal wind anomalies, which measure polar vortex strength. (b) Polar-cap geopotential height anomalies, which are physically linked to vortex strength. (c) Planetary wave-1 amplitude anomalies, which represent large-scale atmospheric waves that disturb the stratosphere. Thin blue lines show yearly values, thick orange lines show 5-year running averages, and green dashed lines show linear trends. Trend magnitudes and corresponding p-values are displayed in each panel. The plots illustrate strong year-to-year variability compared with long-term trends.

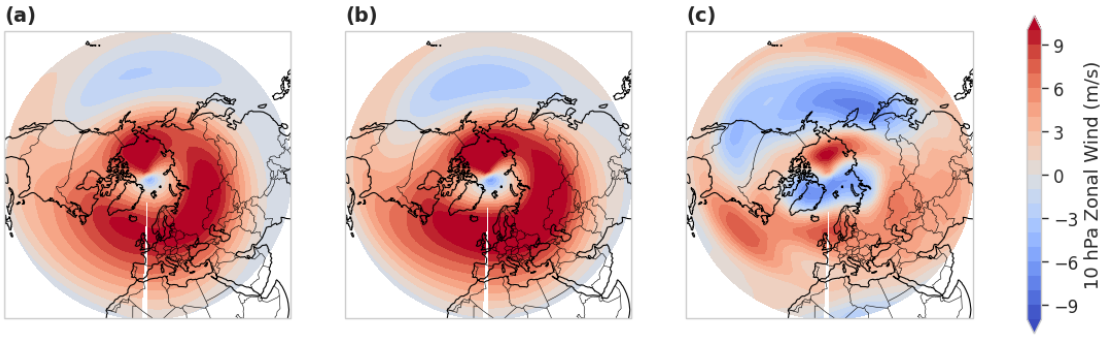

Figure 3: Spatial structure of winter (DJF) zonal wind anomalies at 10 hPa over the Northern Hemisphere polar region. Shading shows wind anomalies (m s^{-1}), with red indicating stronger-than-normal westerlies and blue indicating weaker westerlies or easterly flow. (a) Composite of strong polar vortex years, showing a nearly circular band of enhanced winds around the pole. (b) Another strong vortex state with more longitudinal variation. (c) Composite of weak vortex years, showing reduced winds and clear distortion of the vortex structure. Maps are displayed in polar stereographic projection to emphasize high-latitude patterns.

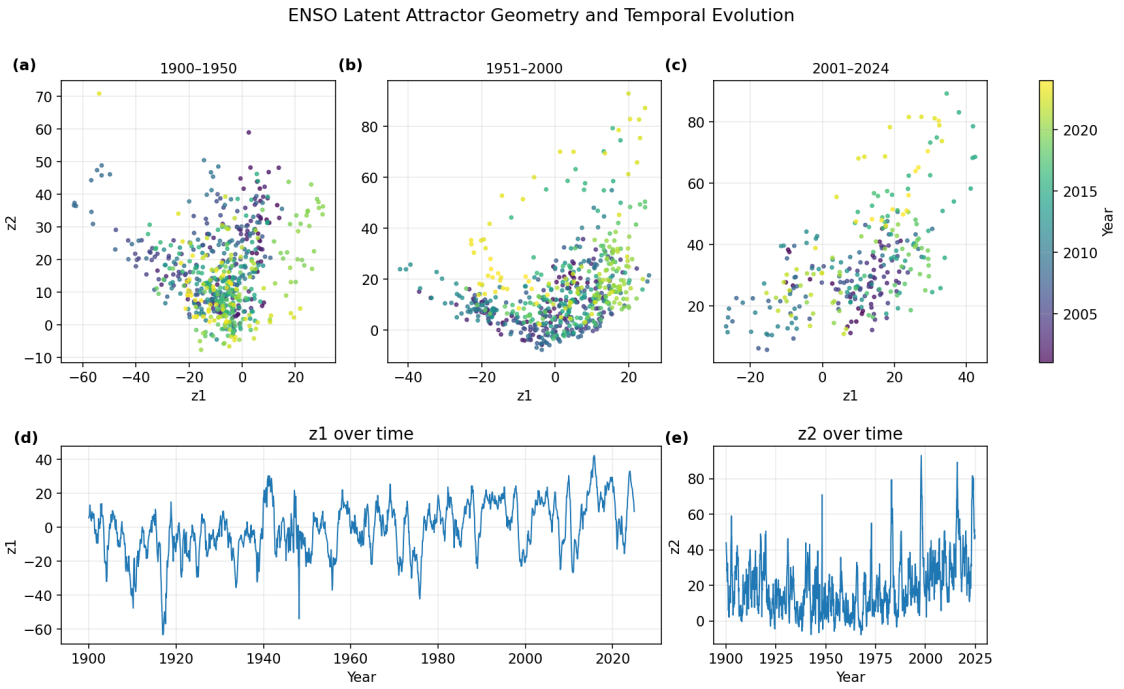

Figure 4: Low-dimensional reconstruction of ENSO variability using PCA followed by nonlinear autoencoder embedding. (a–c) Phase-space plots of the first two latent variables (z_1, z_2) for three periods: 1900–1950, 1951–2000, and 2001–2024. Each point represents one month. The variable z_1 corresponds to ENSO amplitude and is strongly correlated with the El Niño, while z_2 captures changes in spatial structure such as zonal SST gradients. The distribution of points broadens and shifts over time, indicating evolving ENSO behavior. (d) Time series of z_1, showing oscillations between El Niño and La Niña phases. (e) Time series of z_2, showing gradual long-term changes in ENSO spatial structure.

ENSO as a Low-Dimensional System

Figure 4 examines variability in the tropical Pacific using a low-dimensional model. We first reduce the SST data using PCA, then apply a nonlinear autoencoder. The resulting three variables (z_1, z_2, z_3) capture more than 95% of the remaining variance. The first variable, z_1, is strongly correlated with El Niño($r = 0.80$), meaning it represents the main ENSO amplitude signal.

Phase-space plots of (z_1, z_2) for different historical periods show that ENSO does not behave randomly. Instead, the system evolves along a structured surface in this reduced space. Over time, this surface becomes broader and shifts position, especially in the most recent decades (Figs. 4a–c). This indicates that ENSO events are becoming larger and that their spatial structure is changing.

The time series of z_1 (Fig. 4d) shows the familiar oscillation between El Niño and La Niña, with larger swings in recent decades. The second variable, z_2 (Fig. 4e), gradually increases over time, suggesting a shift in how warm and cool anomalies are distributed across the Pacific.

These results show that ENSO can be viewed as motion on a low-dimensional surface whose shape slowly changes over time. This provides a simple way to understand how both the strength and structure of tropical Pacific variability have evolved.

Conclusion

I examined multidecadal changes in large-scale atmospheric circulation, winter stratospheric variability, and the evolving structure of ENSO dynamics. By combining reanalysis diagnostics with

a low-dimensional nonlinear representation of tropical variability, we separated signals that show systematic change from those dominated by internal variability.

In the troposphere, the Hadley cell exhibits statistically significant widening since 1979, with the Southern Hemisphere contributing most strongly to the trend. The Polar cell shows a significant contraction, again primarily in the Southern Hemisphere. In contrast, the Ferrel cell does not display a clear long-term shift. These results indicate that recent circulation changes are spatially uneven and highlight the importance of hemispheric asymmetry in interpreting large-scale climate trends.

In the stratosphere, winter polar vortex diagnostics reveal strong year-to-year variability but no statistically robust long-term trend over 1979–2025. Zonal winds, polar-cap heights, and planetary wave-1 amplitude all fluctuate substantially, suggesting that internal dynamical variability currently dominates over any monotonic forced signal in the Arctic winter stratosphere.

In the tropics, the low-dimensional ENSO reconstruction provides a complementary perspective. ENSO variability can be represented as motion on a structured nonlinear manifold whose geometry evolves over time. The attractor broadens and shifts in recent decades, indicating changes not only in amplitude but also in spatial organization of SST anomalies. This framework highlights that tropical variability may change through gradual modification of dynamical structure rather than through simple linear trends.

Taken together, these findings emphasize that different components of the climate system respond differently over multidecadal timescales. Some features, such as tropical overturning circulation, show measurable structural change, while others, such as the winter stratospheric vortex, remain dominated by variability. Viewing ENSO through a dynamical-systems lens further illustrates that climate change can alter the geometry of variability itself.

Future work should explore how these evolving circulation patterns interact across latitudes, particularly the coupling between tropical variability, midlatitude jets, and stratospheric dynamics. Understanding these connections is essential for improving predictions of regional climate impacts in a warming world.

References

[1] M. P. Baldwin and T. J. Dunkerton. "Stratospheric harbingers of anomalous weather regimes". In: *Science* 294 (2001), pp. 581–584.

[2] A. H. Butler et al. "Defining sudden stratospheric warmings". In: *Bulletin of the American Meteorological Society* 98 (2017), pp. 1027–1042.

[3] K. M. Grise and L. M. Polvani. "The response of midlatitude jets to increased CO2". In: *Geophysical Research Letters* 41 (2014), pp. 7227–7234.

[4] I. M. Held and A. Y. Hou. "Nonlinear Axially Symmetric Circulations in a Nearly Inviscid Atmosphere". In: *Journal of the Atmospheric Sciences* 37 (1980), pp. 515–533.

[5] H. Hersbach, B. Bell, P. Berrisford, et al. "The ERA5 global reanalysis". In: *Quarterly Journal of the Royal Meteorological Society* 146 (2020), pp. 1999–2049.

[6] W. W. Hsieh. "Machine learning methods in the environmental sciences". In: *Cambridge University Press* (2009).

[7] Y. Hu and Q. Fu. "Observed poleward expansion of the Hadley circulation since 1979". In: *Atmospheric Chemistry and Physics* 7 (2007), pp. 5229–5236.

[8] J. Lu, G. A. Vecchi, and T. Reichler. "Expansion of the Hadley cell under global warming". In: *Geophysical Research Letters* 34 (2007), p. L06805.

[9] N. A. Rayner, D. E. Parker, E. B. Horton, et al. "Global analyses of sea surface temperature, sea ice, and night marine air temperature since the late nineteenth century". In: *Journal of Geophysical Research* 108.D14 (2003), p. 4407.

[10] D. J. Seidel et al. "Widening of the tropical belt in a changing climate". In: *Nature Geoscience* 1 (2008), pp. 21–24.

[11] K. E. Trenberth. “The definition of El Niño”. In: *Bulletin of the American Meteorological Society* 78 (1997), pp. 2771–2777.

[12] D. W. Waugh, A. H. Sobel, and L. M. Polvani. “What is the polar vortex and how does it influence weather?” In: *Bulletin of the American Meteorological Society* 98 (2017), pp. 37–44.